Geodesy and Geodynamics 17 (2026) 400–405

Contents lists available at ScienceDirect

Geodesy and Geodynamics

journal homepage: http://www.keaipublishing.com/geog

Research Paper

# Vertical gravity gradient modeling and its influence on gravity datum transfer

Tianxiang Zhou [a], Hongbo Tan [a,*], Guangliang Yang [a], Rugang Xu [b], Xinlin Zhang [a], Jiapei Wang [a], Sheng Liu [a], Hengzhou Meng [a], Ziheng Chen [a]

[a] *Institute of Seismology, China Earthquake Administration, Wuhan 430071, China*
[b] *Anhui Earthquake Agency, Anhui 230031, China*

ARTICLE INFO

*Article history:*
Received 9 August 2025
Received in revised form
16 September 2025
Accepted 19 September 2025
Available online 13 November 2025

*Keywords:*
Gravity adjustment
Gravity gradient
Instrument height correction
Gravity data processing

ABSTRACT

In the past, the free-air gradient $-308.6 \times 10^{-8}$ $s^{-2}$ was used as the vertical gravity gradient of the measuring point in gravity data processing, which resulted in inaccurate instrument height corrections. To investigate the influence of using the vertical gravity gradient, theoretical gradients of the Jinzhai baseline field in the Dabie Mountains were calculated using DEM data and WGM2012 gravity anomaly data. Adjustment results were compared with those using the free-air gradient. Using the theoretically calculated vertical gravity gradient correction improved the scale factor calibration precision by an average of 0.00007. The average precision of gravity adjustment results under different datum controls increased from $2.23 \times 10^{-8}$ $m/s^2$ to $1.45 \times 10^{-8}$ $m/s^2$. In a single-datum control adjustment, the maximum effect of the actual vertical gravity gradient on datum transfer is $8.7 \times 10^{-8}$ $m/s^2$, while the effect without it is as low as $9.0 \times 10^{-8}$ $m/s^2$ and as high as $27.5 \times 10^{-8}$ $m/s^2$. In a multi-datum system, using the actual vertical gravity gradient yields the best results. Even with the three-datum control adjustment, the average effect of the free-air gradient correction on the results reaches $3.9 \times 10^{-8}$ $m/s^2$. Therefore, incorporating measured or theoretically calculated vertical gravity gradients into gravity data processing is essential for significantly enhancing its accuracy and precision.



## 1. Introduction

High-precision gravity data has a wide range of applications, including studying groundwater changes [1,2], studying earthquake precursor information [3–5], and estimating the effective elastic thickness of the lithosphere [5]. Compared to gravity data, gravity gradient data [6,7] contain more high-frequency information and can more accurately reflect the Earth's shallow structural details. Mobile gravity observations in China, which originated in the 1960s and have gradually developed, are the current source for acquiring ground gravity data and monitoring dynamic gravity fields. The development of adjustment processing methods for mobile gravity observations can be divided into two stages. Before the advent of the absolute gravimeter, mobile gravity observations used free network or quasi-stable adjustments [8,9]. After the absolute gravimeter was put into use, gravity adjustments used classical adjustment methods, that is, relative gravity joint measurement under absolute gravity control, with the absolute gravity datum transmitted to each relative gravity joint measurement point to obtain the absolute gravity value of each measurement point.

The process of gravity data preprocessing and adjustment is a crucial step in obtaining high-precision and reliable gravity data. According to the Chinese latest GB/T 20256-2019 "Specifications for the gravimetry control", a series of corrections are generally made to the original mobile gravity observation data, including scale factor correction, solid tide correction, air pressure correction, and instrument height correction. In practical gravity measurement, solid tide correction is primarily performed using either the direct calculation method [10] or the tidal wave component calculation method [11], through which the residuals of the gravity tide [12] term can be controlled within $\pm 2 \times 10^{-8}$ $m/s^2$ by applying theoretical solid tide and ocean tide models. Air pressure correction is based on the measured air pressure value. For instrument

* Corresponding author.
*E-mail address:* thbhong@163.com (H. Tan).

Peer review under the responsibility of Editorial office of Geodesy and Geodynamics.

https://doi.org/10.1016/j.geog.2025.09.006
1674-9847/

height correction, in modern actual gravity measurement, absolute gravity measurement is accompanied by vertical gradient measurement, and the gravity value is corrected to the surface. In relative gravity measurement, the free-air gradient value $-308.6 \times 10^{-8}$ s$^{-2}$ is generally used instead of the actual vertical gravity gradient of the measuring point. Chinese gravity data processing software LGADJ (1990), the open source GRAVS2 (2016), and Gsadjust (2021) developed by the United States Geological Survey all use free-air gradients as vertical gravity gradients when the vertical gravity gradient cannot be measured. Measured data show a difference of $237.6 \times 10^{-8}$ s$^{-2}$ between the Lushan mountainside and Chunshuya [13–15]. Taking the CG5 gravimeter height of 27 cm as an example, the influence of the instrument height correction using the measured gravity vertical gradient value on the segment difference between the two measuring points can reach $64.1 \times 10^{-8}$ m/s$^2$.

The use of free-air gradient can lead to inaccurate instrument corrections, which in turn affect the accuracy of instrument scale factor calibration, network adjustments, and the transfer of absolute gravity datum. Gravity datum transfer refers to transferring the true gravity value measured by the absolute gravimeter through the point difference measured by the relative gravity value to obtain the true gravity value of the measuring point using the relative gravity value. Errors are also transmitted in this process, so studying the influence of vertical gravity gradient on gravity datum transmission can evaluate the precision of gravity data processing results.

With the development of gravity gradiometers [16–18], airborne gravity gradiometers [19–21], satellite gravity gradiometry [22–25], and gravity gradient theory [26–29], as well as the publication of high-precision, high-resolution digital elevation models [30] and gravity field models [31], it has become increasingly possible to obtain the vertical gravity gradient at each measuring point through measurement and theoretical calculation. This paper aims to calculate the disturbance of the vertical gravity gradient caused by terrain and underground density anomalies around the measuring point, based on the 30 m resolution Grid Digital Terrain Model (GDTM) (available for download at http://www.gscloud.cn) and the World Gravity Map 2012 (WGM2012) [32]. The theoretical calculation results of the vertical gravity gradient at each measuring point are closer to the true value than the free-air gradient. The influence of instrument height correction on gravimeter scale factor calibration, adjustment precision, and datum transfer is discussed using the Jinzhai gravity baseline field in the Dabie Mountains as an example, thereby demonstrating the necessity of utilizing a more accurate vertical gravity gradient in future gravity data processing.

## 2. Instrument height correction and gravity gradient

The formula for instrument height correction is as follows:

$$\Delta g = T_{zz} \times h \tag{1}$$

where $h$ is the instrument height, and $T_{zz}$ is the vertical gravity gradient. Since there is no gravity gradient at the measuring point, a free-air gradient value of $-308.6 \times 10^{-8}$ s$^{-2}$ is generally used.

With advances in measurement technology and theory, gravity gradient values can be obtained through various methods at the measuring point, making the continued use of the free-air gradient value inaccurate. Thus, detailed research is required to determine the extent of this inaccuracy and whether a more accurate vertical gravity gradient value is necessary within the current level of instrument precision. Actual vertical gravity gradient values measured in different terrain areas are shown in Table 1 [13–15].

**Table 1**
Comparison of vertical gravity gradients in different terrains.

| Place name | Location | Longitude (°E) | Latitude (°N) | Actual gradient ($\times 10^{-8}$ s$^{-2}$) |
|---|---|---|---|---|
| Jinzhai | Bottom of the mountain | 115.71 | 31.40 | 268.2 |
| | Mountainside | 115.67 | 31.30 | 212.1 |
| | Mountaintop | 115.69 | 31.26 | 301.4 |
| Lushan mountain | Bottom of the mountain | 116.01 | 29.64 | 319.1 |
| | Mountainside | 116.04 | 29.63 | 443.0 |
| | Mountaintop | 115.99 | 29.58 | 310.0 |
| Chunshuya | Col | 110.5 | 31.8 | 205.4 |
| JF, Wuhan | Mountainside | 114.3 | 30.3 | 270.0 |
| IOS, Wuhan | Plains | 114.4 | 30.5 | 308.5 |

The maximum difference is $237.6 \times 10^{-8}$ s$^{-2}$. If the instrument height is 27 cm, the influence of the instrument height correction on the gravity segment difference can reach $64.1 \times 10^{-8}$ m/s$^2$. This difference far exceeds the relative gravity measurement precision level ($1 \times 10^{-7}$ m/s$^2$), significantly affecting the gravity data processing results.

## 3. Theoretical gravity gradient calculation

Both gravity gradient measurement technology and the theory of calculating theoretical gravity gradients have developed rapidly. Modeling methods for calculating gravity and gravity gradients are relatively mature [33–35]. The gravity gradient modeling method is used to calculate the vertical gravity gradient component to study the influence of the vertical gravity gradient on gravity data processing.

Earth's vertical gravity gradient was given as [36]:

$$T_{zz} = A_{zz} + T_{zz}^{\Delta g} + T_{zz}^{\mathrm{Topo}} \tag{2}$$

where $A_{zz}$ is the vertical gradient of the normal gravity field, $T_{zz}^{\Delta g}$ is the vertical gravity gradient anomaly caused by underground gravity anomaly, and $T_{zz}^{\mathrm{Topo}}$ is the vertical gravity gradient anomaly caused by terrain mass.

In this paper, the rectangular gravity gradient model is used to calculate the vertical gravity gradient caused by terrain [37]:

$$T_{zz}^{\mathrm{Pr}} = G\rho \left|\left|\left|\tan^{-1}\frac{xy}{zr}\right|_{x_1}^{x_2}\right|_{y_1}^{y_2}\right|_{z_1}^{z_2} \tag{3}$$

where $x_1, x_2, y_1, y_2, z_1, z_2$ are the coordinates of the corner of the rectangle, $r$ is the spatial distance between the relevant point and the rectangle, $G$ is the gravitational constant, and $\rho$ is the terrain density, which is generally 2.67 g/cm$^3$.

$$r = \sqrt{x^2 + y^2 + z^2} \tag{4}$$

By using a digital elevation model, the large amount of terrain mass is divided into rectangular density bodies, and the effects of all density bodies are superimposed to obtain $T_{zz}^{\mathrm{Topo}} = \sum T_{zz}^{\mathrm{Pr}}$. $T_{zz}^{\Delta g}$ is the vertical gravity gradient anomaly caused by the underground gravity anomaly, calculated using the Fourier transform method [29]:

$$T_{ij}^{\Delta g} = \mathscr{F}^{-1}\{[K(\boldsymbol{k})]G_z(\boldsymbol{k})\} \tag{5}$$

where $G_z(\boldsymbol{k})$ is the vertical gravity in the frequency domain, and $|\boldsymbol{k}| = (k_x^2 + k_y^2)^{1/2}$ represents the inverse Fourier transform, then $T_{zz}^{\Delta g}$ is obtained when $i = j = z$.

$$[K(\boldsymbol{k})] = \begin{bmatrix} -\dfrac{k_x^2}{|\boldsymbol{k}|} & -\dfrac{k_x k_y}{|\boldsymbol{k}|} & -ik_x \\ -\dfrac{k_x k_y}{|\boldsymbol{k}|} & -\dfrac{k_y^2}{|\boldsymbol{k}|} & -ik_y \\ -ik_x & -ik_y & |\boldsymbol{k}| \end{bmatrix} \tag{6}$$

The topographic and underground effects on the actual vertical gravity gradient are calculated using DEM data and Bouguer gravity anomaly data, respectively, and applied to instrument height correction. During gravity data processing, corrections for tide, drift, and air pressure remain unchanged, and the results are obtained after gravity adjustment. The detailed gravity data processing process is shown in Fig. 1.

## 4. Dabie Mountain data comparison

To study the influence of different vertical gravity gradient values for instrument height correction on the processing results of gravity data, we take the measurement data of Jinzhai gravity baseline field in Dabie Mountain as an example [15], reprocess the Dabie Mountain data using the theoretically calculated vertical gravity gradient and conduct a comparative analysis. The Dabie Mountain data used an FG5 absolute gravimeter and two CG6 relative gravimeters to measure absolute gravity and vertical gravity gradient at three gravity datum points. Two complete closed-loop measurements were performed at all points using two CG6 relative gravimeters, where vertical gravity gradient was not measured at the basic points. The measuring points in Dabie Mountains are distributed from the foot to the top of the mountain, with a height difference of 1011.2 m and a gravity segment difference of $225.1 \times 10^{-5}$ m/s$^2$. Among them, A001–A003 are absolute gravity points, and R001–R009 are relative gravity points. The specific measuring point distribution is shown in Fig. 2. In the past, the instrument height correction generally used $-308.6 \times 10^{-8}$ s$^{-2}$ as the free-air gradient value.

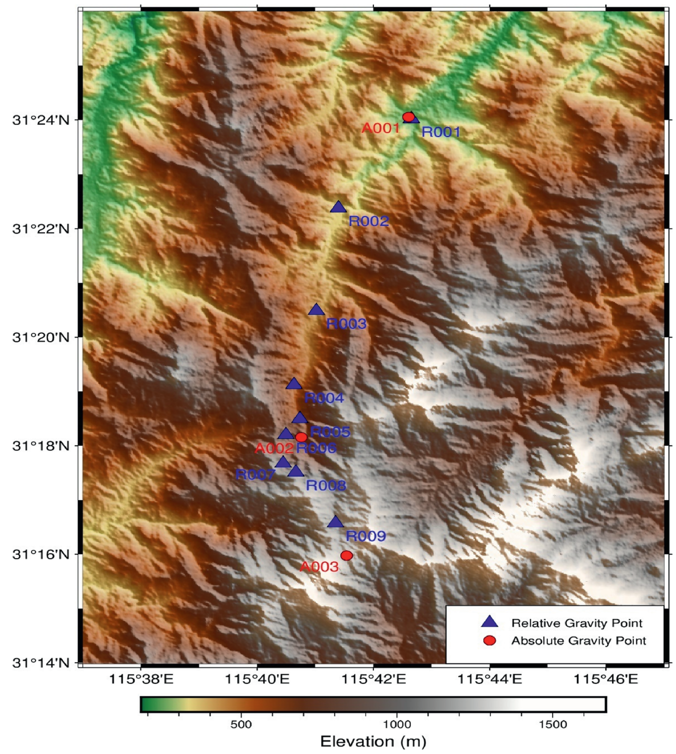


**Fig. 2.** Measurement points distribution map.

This paper uses the Dabie Mountain topographic data with a spatial resolution of 30 m (available for download at http://www.gscloud.cn) and the WGM2012 gravity anomaly data with a resolution of 2' × 2' [32] to calculate the vertical gravity gradient of the Dabie Mountain measuring points. Instrument height corrections were performed using both free-air gradient values and theoretical vertical gravity gradient values, followed by a classical gravity adjustment, and the differences in the results were compared.

Table 2 shows that the average error of the theoretical vertical gravity gradient values at points A001, A002, and A003 is within

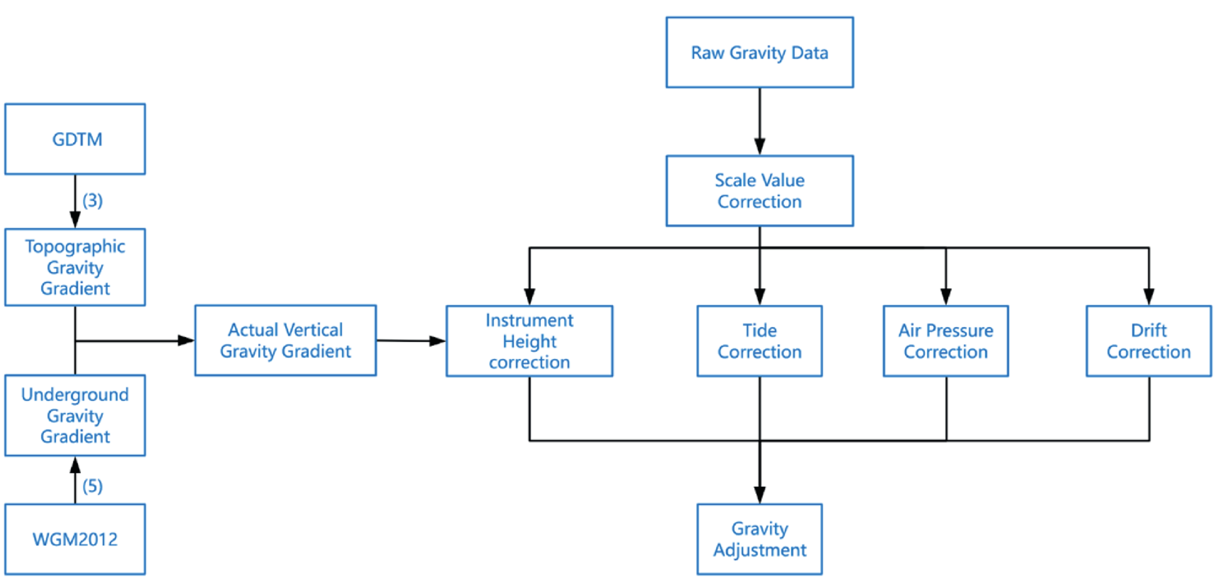


**Fig. 1.** Gravity data processing flow chart.

**Table 2**
Gravity gradient in the Dabie Mountains.

| Measuring point type | Point number | Topographic influence ($\times 10^{-8}$ s$^{-2}$) | Impact of underground density anomalies ($\times 10^{-8}$ s$^{-2}$) | Theoretical gravity gradient ($\times 10^{-8}$ s$^{-2}$) | Measured gravity gradient ($\times 10^{-8}$ s$^{-2}$) |
|---|---|---|---|---|---|
| Gravity datum points | A001 | 42.0 | 3.7 | −255.2 | −268.2 |
| | A002 | 36.1 | 1.1 | −263.8 | −212.1 |
| | A003 | 6.1 | −0.3 | −295.2 | −301.4 |
| Basic gravity points | R001 | 43.1 | 3.7 | −254.2 | — |
| | R002 | 43.0 | 1.9 | −256.7 | — |
| | R003 | 42.3 | 2.5 | −257.2 | — |
| | R004 | 16.8 | 1.9 | −282.3 | — |
| | R005 | 37.7 | 1.4 | −261.9 | — |
| | R006 | 16.2 | 1.4 | −283.4 | — |
| | R007 | 19.1 | 1.0 | −280.5 | — |
| | R008 | 25.2 | 0.5 | −275.3 | — |
| | R009 | 12.8 | −0.6 | −288.8 | — |

10%, with the error at point A002 exceeding 24%. The absolute errors at the other two points are within 5%. This is likely due to the significant influence of a subsurface density anomaly at point A002. The WGM2012 gravity anomaly data have a low resolution and cannot account for the actual influence of subsurface density anomalies in some areas. However, the higher resolution of the terrain data allows for more accurate calculations. In mountainous regions such as the Dabie Mountains, vertical gravity gradient anomalies are primarily influenced by topography, so the overall error of the theoretically calculated vertical gravity gradient is relatively small and reliable. However, in areas where subsurface density anomalies predominate, the theoretically calculated vertical gravity gradient may be less reliable, and actual measurements of the vertical gravity gradient may be necessary. The average difference between the theoretically calculated vertical gravity gradient and the free-air gradient in the Dabie Mountains is $38.6 \times 10^{-8}$ s$^{-2}$. The average instrument height correction at each point increases by $10 \times 10^{-8}$ m/s$^{-2}$. When making instrument height corrections, A001 through A003 use measured vertical gravity gradients, while R001 through R009 use theoretical vertical gravity gradients. This resulting instrument height correction is the closest to the actual result. In the following descriptions, the result using this vertical gravity gradient will be referred to as the actual gravity gradient, while the result using the free-air gradient will be referred to as the general gravity gradient.

Table 3 shows the scale factor calibration results using different vertical gravity gradients. The calculated instrument scale factor calibration precision is between 0.000018 and 0.000050, both exceeding the standard requirement of 0.0005, and the instrument scale factor calibration precision of the entire measuring section is improved by an average of 0.00007.

In subsequent calculations, instrument scale factor calibration values were all corrected using the actual gravity gradient obtained from the three-datum scale factor calibration. Table 4 shows the average precision of the measured points obtained by adjusting using different vertical gravity gradients under different

**Table 4**
Average precision of different datum measuring points.

| Gravity gradient | Points A001, A002 ($\times 10^{-8}$ s$^{-2}$) | Points A001, A003 ($\times 10^{-8}$ s$^{-2}$) | Points A002, A003 ($\times 10^{-8}$ s$^{-2}$) | Points A001, A002, A003 ($\times 10^{-8}$ s$^{-2}$) |
|---|---|---|---|---|
| Actual gravity gradient | 1.5 | 1.4 | 1.4 | 1.3 |
| General gravity gradient | 2.3 | 2.1 | 2.1 | 2.1 |

datum points. The results in Table 4 show that the precision of the results using the actual gravity gradient is generally superior to that using the general gravity gradient. The average precision of the results under different datum increases from $2.23 \times 10^{-8}$ m/s$^2$ to $1.45 \times 10^{-8}$ m/s$^2$. It is further demonstrated that the use of actual gravity gradient correction can effectively improve adjustment precision, and that the adjusted gravity values are brought closer to the true gravity values through its application, which is of great significance for studying the Earth's gravity field.

To further investigate the influence of gravity gradient on datum transfer, adjustments were performed using different gravity gradients and a single datum. Three absolute point gravity values from the adjustment results were selected and subtracted from the absolute point datum values. The final results are shown in Table 5. The results in Table 5 show that the results obtained using the A002 point control under the actual gravity gradient correction are the best, and the results using the actual gravity gradient correction are generally superior to those using the general gravity gradient. The absolute point datum value can be considered as the "true value" relative to the relative gravity measurement value. The maximum difference between the result using the general gravity gradient and the true value is $27 \times 10^{-8}$ m/s$^2$, while the maximum difference between the result using the actual gravity gradient and the true value is $8.7 \times 10^{-8}$ m/s$^2$. From this respect, the use of the actual gravity gradient result is far more reliable than the use of the general gravity gradient result.

Gravity adjustment results obtained using actual gravity gradients for instrument height correction and three-datum scale factor calibration are theoretically the most reliable and can be considered the "true value" of the measurement point. The "true value" was subtracted from the gravity values obtained using other

**Table 5**
Comparison of error propagation results under different datum points using different gravity gradients.

| Gravity gradients | Point number | Point A001 ($\times 10^{-8}$ s$^{-2}$) | Point A002 ($\times 10^{-8}$ s$^{-2}$) | Point A003 ($\times 10^{-8}$ s$^{-2}$) |
|---|---|---|---|---|
| Actual gravity gradient | A001 | 0 | −6.5 | 2.3 |
| | A002 | 6.5 | 0 | 8.7 |
| | A003 | 2.1 | −8.7 | 0 |
| General gravity gradient | A001 | 0 | −18.4 | 9.0 |
| | A002 | 18.4 | 0 | 27.5 |
| | A003 | −9.0 | −27.5 | 0 |

**Table 3**
Results of different base scale factor calibration values.

| Instrument name | Gravity gradient | Points A001, A002 | Points A001, A003 | Points A002, A003 | Points A001, A002, A003 |
|---|---|---|---|---|---|
| CG6-090 | Actual gravity gradient | 1.000024 ± 0.000023 | 1.000171 ± 0.000018 | 0.999775 ± 0.000026 | 1.000181 ± 0.000019 |
| | General gravity gradient | 1.000382 ± 0.000050 | 1.000169 ± 0.000038 | 0.999973 ± 0.000048 | 1.000158 ± 0.000033 |
| CG6-092 | Actual gravity gradient | 0.999909 ± 0.000023 | 0.999839 ± 0.000018 | 1.000114 ± 0.000026 | 0.999849 ± 0.000019 |
| | General gravity gradient | 1.000029 ± 0.000050 | 0.999815 ± 0.000038 | 0.999618 ± 0.000048 | 0.999804 ± 0.000033 |

**Table 6**
Differences between different adjustments and the "true value".

| Point number | Points A001, A002 | | Points A001, A003 | | Points A002, A003 | | Points A001, A002, A003 |
|---|---|---|---|---|---|---|---|
| | General results ( $\times 10^{-8}$ m $s^{-2}$) | Actual results ( $\times 10^{-8}$ m $s^{-2}$) | General results ( $\times 10^{-8}$ m $s^{-2}$) | Actual results ( $\times 10^{-8}$ m $s^{-2}$) | General results ( $\times 10^{-8}$ m $s^{-2}$) | Actual results ( $\times 10^{-8}$ m $s^{-2}$) | General results ( $\times 10^{-8}$ m $s^{-2}$) |
| A001 | 0.1 | 0 | 0 | 0 | 13.5 | 5 | 0.1 |
| R001 | 4.4 | 0.6 | 8.2 | 3.6 | 7.4 | 1.9 | 2.2 |
| R002 | 4.9 | 0.6 | 7.6 | 3.6 | 7.9 | 1.9 | 2.8 |
| R003 | 5 | 0.6 | 7.5 | 3.6 | 8 | 1.9 | 2.9 |
| R004 | 10.4 | 0.7 | 2.1 | 3.5 | 13.4 | 1.9 | 8.2 |
| R005 | 6 | 0.6 | 6.5 | 3.6 | 9 | 1.8 | 3.9 |
| A002 | 0 | 0 | 20.4 | 6.9 | 0 | 0.1 | −0.1 |
| R006 | 10.5 | 0.6 | 2.1 | 3.6 | 13.5 | 1.9 | 8.3 |
| R007 | 9.9 | 0.7 | 2.6 | 3.5 | 12.9 | 1.9 | 7.8 |
| R008 | 8.8 | 0.6 | 3.7 | 3.6 | 11.8 | 1.9 | 6.7 |
| R009 | 13.9 | 2.9 | 1.6 | 2 | 7.3 | 1.1 | 4.3 |
| A003 | 19.6 | 5.9 | 0 | 0 | 0.1 | 0 | 0 |
| Average value | 7.8 | 1.2 | 5.2 | 3.1 | 8.7 | 1.8 | 3.9 |

adjustment methods. The results are shown in Table 6. The results in Table 6 show that the average difference between the actual gravity gradient results and the "true value" when using only two-datum for control is $3.1 \times 10^{-8}$ m/s$^2$, with a minimum of only $1.23 \times 10^{-8}$ m/s$^2$. In contrast, the average difference using the general gravity gradient results is $3.9 \times 10^{-8}$ m/s$^2$ when using three datum points, and a maximum of $8.7 \times 10^{-8}$ m/s$^2$ when using two datum points. Overall, the differences are smaller near the datum and larger far from it, primarily due to the effects of error propagation. The Jinzhai data set in the Dabie Mountains has 12 points, a quarter of which are datum points, so the influence of error propagation is relatively small. However, in a complex survey network with a smaller proportion of datum points, differences in vertical gravity gradients may have a greater influence on the results of the entire network. This requires further research.

## 5. Conclusion

Historically, the free-air gradient was conventionally employed for instrument height corrections due to the practical challenges in acquiring measured vertical gravity gradients. This approach provided a good approximation when the actual gravity gradient at the measuring point was unavailable. This method has been used for processing mobile gravity measurements since the 1960s. With the development of technology and theory since the 21st century, more methods have become available for measuring or modeling vertical gravity gradients, making it feasible to use the actual vertical gravity gradient at the measuring points in future gravity data processing.

This paper calculates vertical gravity gradients using a DEM model and a Bouguer gravity anomaly model (with terrain correction). Based on the theoretical vertical gravity gradients calculated in this paper, the influence of the vertical gravity gradient on the relative gravimeter scale factor calibration, the adjustment results, and the gravity datum transfer is investigated.

Judging from the results of scale factor calibration, the scale factor precision of the entire measuring section is improved by an average of 0.00007. From the perspective of the precision of the adjustment results, the precision of the results using the actual vertical gravity gradient is generally better than that using the general gravity gradient results. The average precision of the results of different datum points can be improved from $2.23 \times 10^{-8}$ m/s$^2$ to $1.45 \times 10^{-8}$ m/s$^2$. Most importantly, the influence of the gravity gradient on the gravity datum transfer is studied. Although the average value of the gravity gradient change in the Dabie Mountains is $23.4 \times 10^{-8}$ s$^{-2}$, which is much smaller than the maximum difference of $237.6 \times 10^{-8}$ s$^{-2}$ in Table 1, the resulting influence on the results is also not negligible. In the case of single-datum control adjustment, the maximum influence of the actual vertical gravity gradient on the datum transfer is $8.7 \times 10^{-8}$ m/s$^2$, while the influence of not using it is the smallest at $9.0 \times 10^{-8}$ m/s$^2$ and the largest at $27.5 \times 10^{-8}$ m/s$^2$. Although the single-datum control effect is poor, this result also illustrates the huge influence of the gravity gradient on the datum transfer. In the case of multi-datum, the average difference between the results using the actual vertical gravity gradient and the "true value" is the smallest. Even under the three-datum control condition, the average difference between the results calculated using the free-air gradient and the "true value" reached $3.9 \times 10^{-8}$ m/s$^2$.

The vertical gravity gradient at a measuring point is most reliably obtained through direct measurement using a gravity gradiometer, although this method is relatively expensive; alternatively, it can be effectively calculated using theoretical models. However, due to the low resolution of gravity anomaly data, the calculated results may be significantly biased in areas where gravity gradient anomalies caused by subsurface density anomalies dominate. Topographic resolution can reach 30 m or higher, so using theoretically calculated vertical gravity gradient should be more reliable in mountainous areas where topographically driven gravity gradient anomalies dominate. According to this analysis, vertical gravity gradients may have a greater influence on regional and even national gravity networks. Eliminating these effects can yield more accurate and reliable gravity data, thereby serving and promoting relevant Earth science research and development. These issues require further research.

## CRediT authorship contribution statement

**Tianxiang Zhou:** Writing – original draft. **Hongbo Tan:** Writing – review & editing, Writing – original draft. **Guangliang Yang:** Writing – review & editing. **Rugang Xu:** Writing – review & editing. **Xinlin Zhang:** Writing – review & editing. **Jiapei Wang:** Writing – review & editing. **Sheng Liu:** Writing – review & editing. **Hengzhou Meng:** Writing – review & editing. **Ziheng Chen:** Writing – review & editing.

## Declaration of competing interest

The authors declare that there is no conflicts of interest.

## Acknowledgements

We gratefully acknowledge the financial support of the National Natural Science Foundation of China (42174104); the Special Project for Basic Resources Survey of the Ministry of Science and Technology (2023FY10150502); the Natural Science Foundation of Hubei Province (2022CFB350); the Key Project of the National Natural Science Foundation of China (U1939204); the Spark Program of Earthquake Science and Technology (XH23014YC); and Hubei Province Natural Science Foundation, NO. 2025AFB854.

## References

[1] B. Creutzfeldt, A. Güntner, H. Wziontek, et al., Reducing local hydrology from high-precision gravity measurements: a lysimeter-based approach, Geophys. J. Int. 183 (1) (2010) 178–187, https://doi.org/10.1111/j.1365-246X.2010.04742.x.
[2] J. Kennedy, T.P.A. Ferré, A. Güntner, et al., Direct measurement of subsurface mass change using the variable baseline gravity gradient method, Geophys. Res. Lett. 41 (8) (2014) 2827–2834, https://doi.org/10.1002/2014GL059673.
[3] F. Zhan, Y. Zhu, J. Ning, et al., Gravity changes before large earthquakes in China: 1998–2005, Geo-spatial, Inf. Sci. 14 (1) (2011) 1–9, https://doi.org/10.1007/s11806-011-0440-0.
[4] C. Shen, Y. Zhu, M. Hu, et al., Time-varying gravity field monitoring and strong earthquake prediction on the Chinese mainland, Earthq. Res. China 36 (4) (2020) 729–743.
[5] J.F. Kirby, Estimation of the effective elastic thickness of the lithosphere using inverse spectral methods: the state of the art, Tectonophysics 631 (2014) 87–116, https://doi.org/10.1016/j.tecto.2014.04.021.
[6] X. Gao, D. Huang, Research on 3D focusing inversion of gravity gradient tensor data based on a conjugate gradient algorithm, Chin. J. Geophys. 60 (4) (2017) 1571–1583, https://doi.org/10.6038/cjg20170429 (in Chinese).
[7] P. Qin, D. Huang, Integrated gravity and gravity gradient data focusing inversion, Chin. J. Geophys. 59 (6) (2016) 2203–2224, https://doi.org/10.6038/cjg20160624 (in Chinese).
[8] H. Li, D. Liu, S. Liu, et al., Integrated adjustment models for the seismic-gravity network, Crustal Deform. Earthq. 11 (Sup) (1991) 68–74.
[9] H. Li, G. Fu, S. Sun, et al., Computation on dynamic gravity changes in the Western area of Yunnan province, Crustal Deform. Earthq. (2000) 60–66, https://doi.org/CNKI:SUN:DKXB.0.2000-01-009.
[10] I.M. Longman, Formulas for computing the tidal accelerations due to the moon and the sun, J. Geophys. Res. 64 (12) (1959) 2351–2355, https://doi.org/10.1029/JZ064i012p02351.
[11] Y. Tamura, A harmonic development of the tide-generating potential, Marees Terr. Bull. d'Info. 99 (1987) 6813–6855.
[12] H. Tan, O. Francis, G. Wu, et al., Evaluation of global ocean tide models based on tidal gravity observations in China, Geod, Geodyn. 12 (6) (2021) 451–458, https://doi.org/10.1016/j.geog.2021.08.001.
[13] Z. Chen, H. Li, L. Xing, et al., Study on non-linear variation of vertical gradient of gravity, J. Geodesy Geodyn. 34 (2) (2014) 27–30, https://doi.org/10.14075/j.jgg.2014.02.018.
[14] L. Xing, L. Wang, S. Sun, et al., Determination of gravity values for lushan short gravity calibration baseline, J. Geodesy Geodyn. 36 (9) (2016) 753–756, https://doi.org/10.14075/j.jgg.2016.09.001.
[15] R. Xu, X. Zhang, X. Liang, et al., Analysis for synthetic adjustment of absolute and relative gravity at the Jinzhai gravity baseline in Dabie Mountain, Seismol. Geol. 45 (5) 1147–1169, https://doi.org/10.3969/j.issn.0253-4967.2023.05.007.
[16] D. DiFrancesco, A. Grierson, D. Kaputa, et al., Gravity gradiometer systems–advances and challenges, Geophys. Prospect. 57 (4) (2009) 615–623, https://doi.org/10.1071/ASEG2007ab034.
[17] C. Jekeli, A review of gravity gradiometer survey system data analyses, Geophysics 58 (4) (1993) 508–514, https://doi.org/10.1190/1.1443433.
[18] M.V. Moody, H.A. Chan, H.J. Paik, Superconducting gravity gradiometer for space and terrestrial applications, J. Appl. Phys. 60 (12) (1986) 4308–4315, https://doi.org/10.1063/1.337474.
[19] Z. Zhang, J. Shi, Z. Yu, et al., Feasibility analysis of submarine detection method based on the airborne gravity gradient, in: 2018 37th Chinese Control Conference (CCC), IEEE, 2018, pp. 4587–4591.
[20] R. Forsberg, A.V. Olesen, Airborne Gravity Field Determination, Sciences of geodesy-I: Advances and Future Directions, 2010, pp. 83–104, https://doi.org/10.1007/978-3-642-11741-1_3.
[21] C. Jekeli, Airborne gradiometry error analysis, Surv. Geophys. 27 (2) (2006) 257–275, https://doi.org/10.1007/s10712-005-3826-4.
[22] J. Bouman, J. Ebbing, M. Fuchs, et al., Satellite gravity gradient grids for geophysics, Sci. Rep. 6 (1) (2016) 21050, https://doi.org/10.1038/SREP21050.
[23] R. Rummel, O.L. Colombo, Gravity field determination from satellite gradiometry, Bull. Geod. 59 (1985) 233–246, https://doi.org/10.1007/BF02520329.
[24] J. Bouman, W. Bosch, J. Sebera, Assessment of systematic errors in the computation of gravity gradients from satellite altimeter data, Mar. Geod. 34 (2) (2011) 85–107, https://doi.org/10.1080/01490419.2010.518498.
[25] B. Wu, Y. Qiu, Q. Yang, et al., Research on ultra-stable platform technologies of gravitational gradiometry satellite, Adv. Small Satell. Technol. 1 (4) (2024) 1–7, https://doi.org/CNKI:SUN:AXWX.0.2024-04-001 (in Chinese).
[26] M. Talwani, Computation with the help of a digital computer of magnetic anomalies caused by bodies of arbitrary shape, Geophysics 30 (5) (1965) 797–817, https://doi.org/10.1190/1.1439654.
[27] C.J. Montana, K.L. Mickus, W.J. Peeples, Program to calculate the gravitational field and gravity gradient tensor resulting from a system of right rectangular prisms, Comput. Geosci. 18 (5) (1992) 587–602, https://doi.org/10.1016/0098-3004(92)90096-A.
[28] S. Rózsa, G. Tóth, Prediction of Vertical Gravity Gradients Using Gravity and Elevation Data, A Wind. Futur. Geod., 2005, pp. 344–349, https://doi.org/10.1007/3-540-27432-4_59.
[29] K.L. Mickus, J.H. Hinojosa, The complete gravity gradient tensor derived from the vertical component of gravity: a Fourier transform technique, J. Appl. Phys. 46 (3) (2001) 159–174, https://doi.org/10.1016/S0926-9851(01)00031-3.
[30] Z. Li, P. Li, D. Ding, et al., Research progress of global high resolution digital elevation models, Geomat, Inf. Sci. Wuhan Univ. 43 (12) (2018) 1927–1942, https://doi.org/10.13203/j.whugis20180295.
[31] B. Bucha, J. Janák, J. Papčo, et al., High-resolution regional gravity field modelling in a mountainous area from terrestrial gravity data, Geophys. Suppl. Mon. Not. R. Astron. Soc. 207 (2) (2016) 949–966, https://doi.org/10.1093/gji/ggw311.
[32] S. Bonvalot, A. Briais, M. Kuhn, et al., Global Grids : World Gravity Map (WGM2012), Bureau Gravimetrique International, 2012.
[33] M. Okabe, Analytical expressions for gravity anomalies due to homogeneous polyhedral bodies and translations into magnetic anomalies, Geophysics 44 (4) (1979) 730–741, https://doi.org/10.1190/1.1440973.
[34] H.J. Götze, B. Lahmeyer, Application of three-dimensional interactive modeling in gravity and magnetics, Geophysics 53 (8) (1988) 1096–1108, https://doi.org/10.1190/1.1442546.
[35] L. Yao, C. Yao, Forward modeling of gravity, gravity gradients, and magnetic anomalies due to complex bodies, J. China Univ. Geosci. 18 (3) (2007) 280–286, https://doi.org/10.1016/S1002-0705(08)60008-4.
[36] O. Odalovic, K. Medved, S. Naod, Modeling of vertical gravity gradient by normal gravity field and digital terrain models, J. Geod. 96 (10) (2022) 74, https://doi.org/10.1007/s00190-022-01669-y.
[37] D. Nagy, G. Papp, J. Benedek, The gravitational potential and its derivatives for the prism, J. Geod. 74 (2000) 552–560, https://doi.org/10.1007/s001900000116.

**Tianxiang Zhou**, Master Candidate, Student of the Department of Geophysics at the Institute of Seismology, China Earthquake Administration. His research interests include gravity data processing and geophysical field structure inversion. His work includes optimizing relative gravity data adjustment methods, optimizing gravity data processing, and inverting three-dimensional temperature field structure.